Settling of a particle pair through a sharp, miscible density interface

David Deepwell,[1,*] Raphael Ouillon,[2] Eckart Meiburg,[3] and Bruce R. Sutherland[1]
[1]*Department of Physics, University of Alberta, Edmonton, Alberta T6G 2E1, Canada*
[2]*Department of Mechanical Engineering, Massachusetts Institute of Technology, Cambridge, Massachusetts 02139, USA*
[3]*Department of Mechanical Engineering, University of California, Santa Barbara, Santa Barbara, California 93106, USA*

(Received 23 September 2020; accepted 30 March 2021; published 20 April 2021)

We perform numerical simulations to examine settling and fluid transport by a pair of particles passing through a thin density interface of a two-layer fluid. As the particles settle through the interface, they deform the interface and carry upper layer fluid into the lower layer. This increased buoyancy hinders the particle settling such that the trailing particle collides with the leading particle at strong stratification and when the particles are nearly vertically aligned. When descending into the lower layer, the upper layer fluid detaches from the particles, returning upward within a wake whose width is on the order of two particle diameters. Due to the added buoyancy and the returning wake, particle settling is hindered and the trailing particle separates away from the leading particle when aligned within or near the wake of the leading particle. Meanwhile, the trailing particle re-entrains fluid detached from the leading particle. Consequently, the transport of upper layer fluid into the lower layer increased by up to 40% in the case of weak stratification.

DOI: 10.1103/PhysRevFluids.6.044304

I. INTRODUCTION

The settling of particles such as silt, clay, and organic matter in density stratified environments commonly occurs in the ocean, especially in estuaries where rivers are an important influx to the coastal oceans of terrestrial matter and fresh water. Dense suspended terrestrial matter settles from the fresh surface layer into the saline lower layer and eventually onto the seafloor. In the ocean, the settling of suspended particles is the primary driver of vertical mass flux [1], although the settling is delayed and an accumulation of the settling material, such as marine snow [2–4] or plankton [5], occurs in the presence of a density interface. Recently, there has been great interest in modeling the physical processes of microplastic transport within the ocean, especially in regard to its settling and deposition [6–8].

The settling dynamics are surprisingly complex, as revealed by laboratory experiments [9,10]. As particles settle, they drag some of the surrounding fluid with it, resulting in a net vertical displacement of upper layer fluid to depth. A recent review of this and other particle settling effects can be found in Magnaudet and Mercier [11]. The vertical displacement of fluid carried by a large number of particles in the surface transition layer has been suggested as a sizable source of diapycnal mixing [12,13]. In the context of a particle-bearing surface gravity current, Sutherland *et al.* [10] demonstrated that the collective settling of these particles, even at concentrations as low as 2.5%, caused the advance of the current to come to a near stop because of the large amount of interstitial fluid being carried out of the current by the particles as they settled to depth. It was hypothesized

*deepwell@ualberta.ca

that collective settling behavior enhanced the transport of fluid from the current to depth. As a step toward understanding this collective settling phenomenon, especially in regard to the efficacy of fluid transport, here we present numerical simulations of the interaction of pairs of particles as they pass through a density interface.

The settling of an individual particle through a stratified environment is hindered by the increased buoyancy caused by the dragging of lighter fluid surrounding the particle [14], the shedding of vortices [15], the formation of a trailing jet [16], or the formation of internal waves [17]. Settling may be further hindered for porous particles which require diffusive exchange of interstitial and ambient fluid [18,19]. This hindered settling is evident by a minimum settling speed as the particle passes through the interface [20,21]. At high Reynolds number, the settling of the particle may even stop and reverse directions [22]. To explain the hindering, Verso *et al.* [23] created a modified Maxey-Riley-type model accounting for the stratification effects in the particle settling, in which an exponentially decaying body force was added to account for a captured upper layer fluid surrounding the particle. The fluid drift volume caused by a single settling particle has been explored for homogeneous fluids [24,25], linearly stratified fluids [26,27], and for a particle crossing an interface [20,21].

In a homogeneous fluid, two settling spherical particles at moderate Reynolds number experience different phases of interaction, collectively called drafting-kissing-tumbling. This chaotic sequence of phases consist of the trailing particle drafting within the wake of the leading particle until coming in contact before separating again [28–32]. At low Reynolds number, theory [33–36] and experiments [37,38] demonstrate that two settling particles interact to enhance their collective settling speed while experiencing a lateral drift when the particles are neither vertically nor horizontally aligned but remain approximately equal in separation.

As far as we are aware, Doostmohammadi and Ardekani [39] is the only investigation of particle pair settling in a stratified environment. For a linearly stratified fluid at moderate Reynolds number, they observed that two spherical particles settling side by side had an attractive force while they settled, as opposed to the readily observed separation of particles in a homogeneous fluid. The authors showed that the homogeneous stages of drafting-kissing-tumbling became drafting-kissing-separating in which the kissing stage was prolonged.

The paper presented here provides an examination of the low Reynolds number settling of a pair of particles through an interface with thickness comparable to the particle size. We use numerical simulations to model the settling of a pair of equal radii spherical particles and to examine the deformation of the density field caused by the pair as they pass through the interface. We have focused on somewhat low Reynolds numbers ($\mathrm{Re} = 1/4$) for which particles are either small or the settling velocity is slow, as could be caused by the particle density being similar to that of the surrounding fluid. In Sec. II, we describe the numerical methods and initial particle and density setup. Section III presents both qualitative and quantitative descriptions of the particles settling and horizontal drift velocities, separation, and entrainment of upper layer fluid as it depends on particle orientation, separation, and the strength of the stratification. We summarize our findings in Sec. IV with predictions on the interactions of larger clusters of particles in a stratified medium.

II. INITIAL CONDITIONS AND NUMERICAL MODEL

We consider the settling of a pair of identical particles from one homogeneous layer into a denser, lower layer through a continuous thin density interface (Fig. 1). The particles were spheres with density ρ_p, diameter D_p, and were initially located at rest within the upper layer of a two-layer fluid. The particles were initially situated such that they were separated by a distance s_0 between their closest points and the angle between the line connecting their centers and the vertical was θ. The particle separation distance and orientation angle varied within the ranges $s_0/D_p \in [1, 7]$ and $\theta \in [0^\circ, 90^\circ]$, respectively. Because we are interested in how the density field may cause particles to approach each other, possibly colliding to form larger aggregate structures, many of the results will use $s_0/D_p = 2$ for which the particles are close.

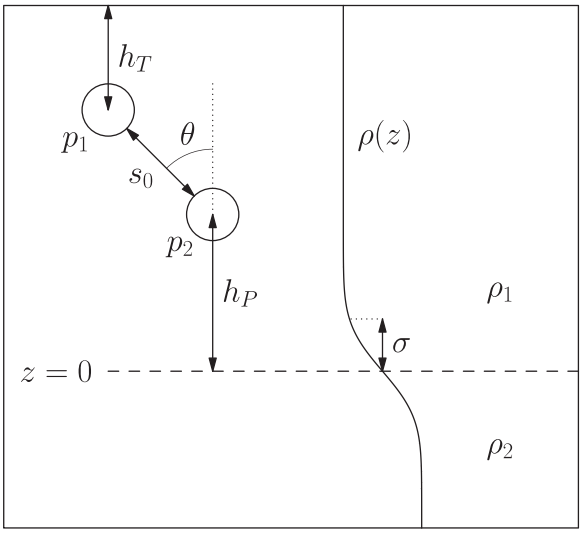

FIG. 1. Schematic of initial conditions. Dimensions are not to scale.

Setting the origin of the vertical axis at the center of the interface, the initial background density stratification was described by

$$\rho(z) = \rho_1 + \frac{\Delta\rho}{2}[1 - \mathrm{erf}(z/\sigma)], \tag{1}$$

where $\Delta\rho = \rho_2 - \rho_1$ is the density difference between the lower and upper layers. The half-width of the pycnocline was the particle diameter, $\sigma = D_p$. This relatively thin transition from upper to lower layer fluid was advantageous to quantify fluid transport from the upper to lower layer while also ensuring the interface was well-resolved.

We solved the Navier-Stokes equations under the Boussinesq approximation for an incompressible fluid,

$$\frac{D\mathbf{u}}{Dt} = -\frac{1}{\rho_1}\nabla p + \frac{\rho}{\rho_1}\mathbf{g} + \nu\nabla^2\mathbf{u} + \mathbf{f}_{\mathrm{IBM}}, \tag{2a}$$

$$\nabla \cdot \mathbf{u} = 0, \tag{2b}$$

$$\frac{D\rho}{Dt} = \kappa\nabla^2\rho, \tag{2c}$$

in which $\mathbf{u} = (u, v, w)$ is the velocity vector, p is the pressure, $\mathbf{g}$ is the acceleration vector due to gravity, ν is the kinematic viscosity, and κ is the molecular diffusivity. The motion of the particles imparts momentum to the background fluid through the numerical body force $\mathbf{f}_{\mathrm{IBM}}$, implemented using the immersed boundary method (IBM) [40,41]. $\mathbf{f}_{\mathrm{IBM}}$ is a fictitious force that imposes the desired no-slip boundary condition on the surface of the particles. Details on the multistep process of calculating $\mathbf{f}_{\mathrm{IBM}}$ can be found in Kempe and Fröhlich [42].

The variables in Eqs. (2) were nondimensionalized (primed variables) as follows:

$$\mathbf{u} = w_s\mathbf{u}', \qquad p = \rho_1 w_s^2 p',$$
$$\mathbf{x} = D_p\mathbf{x}', \qquad \rho = \rho_1 + \Delta\rho\rho',$$
$$t = \tau t',$$

where

$$w_s = \frac{1}{18}\frac{\rho_p - \rho_1}{\rho_1}\frac{gD_p^2}{\nu}$$

is the Stokes settling velocity within the upper layer and $\tau = D_p/w_s$ is the characteristic timescale.

In nondimensional form, the governing equations are

$$\frac{D\mathbf{u}'}{Dt'} = -\boldsymbol{\nabla} p' + \frac{1}{Fr^2}\rho'\mathbf{k} + \frac{1}{\mathrm{Re}}\nabla^2\mathbf{u}' + \mathbf{f}'_{\mathrm{IBM}}, \tag{3a}$$

$$\boldsymbol{\nabla}\cdot\mathbf{u}' = 0, \tag{3b}$$

$$\frac{D\rho'}{Dt'} = \frac{1}{\mathrm{Pe}}\nabla^2\rho', \tag{3c}$$

where the following nondimensional parameters govern the dynamics of the fluid phase,

$$\mathrm{Fr} = \frac{w_s}{ND_p} \qquad \text{Froude number,}$$

$$\mathrm{Re} = \frac{w_s D_p}{\nu} \qquad \text{Reynolds number,}$$

$$\mathrm{Sc} = \frac{\nu}{\kappa} \qquad \text{Schmidt number,}$$

$$\mathrm{Pe} = \mathrm{ReSc} = \frac{w_s D_p}{\kappa} \qquad \text{Péclet number,}$$

and the characteristic buoyancy frequency is defined as

$$N^2 = \frac{g\Delta\rho}{D_p\rho_1}.$$

We have predominantly used a Reynolds number of $1/4$ which lies outside what is classified as Stokesian. This larger value of Re was selected because of the cheaper computational costs compared to that with lower Reynolds numbers. The time step was two orders of magnitude larger and took approximately half the wall clock time for $\mathrm{Re} = 1/4$ compared to $\mathrm{Re} = 1/16$ when used with the same computational resources. With this dramatic difference in timescales, it would have been unfeasible to attempt the number of simulations we completed at a smaller Reynolds number. Comparison of different Reynolds numbers will be made in Sec. III G. To maintain the relatively thin density interface for the duration of the simulation, the Schmidt number was that for a salt stratified fluid, $\mathrm{Sc} = 700$, resulting in $\mathrm{Pe} = 175$. Following Inman *et al.* [26], the density boundary layer thickness is estimated as $\delta_d/D_p \sim \mathrm{Pe}^{-1/3} \approx 0.18$, which is approximately four times the grid spacing. Although this boundary layer is only marginally resolved, the bulk properties of the particle settling and interaction with the density stratification are found to be correct. Verification of the model for the present configuration is made in Appendix A by comparing the sedimentation of a single particle to previous experimental studies of particle sedimentation in homogeneous and stratified fluids.

Rather than using the Froude number to characterize the strength of the stratification, we use the ratio of the difference of the particle density to the densities of each layer:

$$\Gamma = 1 - \frac{\rho_p - \rho_2}{\rho_p - \rho_1} = \frac{\rho_2 - \rho_1}{\rho_p - \rho_1}. \tag{4}$$

With this definition, $\Gamma = 0$ for a homogenous fluid ($\rho_1 = \rho_2$) and $\Gamma = 1$ if the particles are neutrally buoyant in the lower layer ($\rho_p = \rho_2$). In this way, the relative strength of the stratification to the particle density is made evident. In the following, we run simulations where $\Gamma \in [0, 0.7]$. Values of $\Gamma > 0.7$ were prohibitively computationally expensive due to both the decreased grid spacing

necessary to resolve the sharp gradients of density as the particles settle through the interface and due to the long time required for particles to descend within the lower layer.

The motion of a particle is described by

$$m_p \frac{d\mathbf{u}_p}{dt} = \oint_{\Gamma_p} \tau_h \cdot \mathbf{n} dA + V_p(\rho_p - \rho_1)\mathbf{g} + \mathbf{F}_{c,p}, \tag{5a}$$

$$I_p \frac{d\omega_p}{dt} = \oint_{\Gamma_p} \mathbf{r} \times (\tau_h \cdot \mathbf{n}) dA + \mathbf{T}_{c,p}, \tag{5b}$$

where m_p is the mass of the particle, τ_h is the hydrodynamic stress tensor, V_p is the volume of the particle, I_p is the moment of inertia, and $\mathbf{r}$ is the radial vector from the center of the particle. $\mathbf{F}_{c,p}$ and $\mathbf{T}_{c,p}$ are the forces and torques arising due to particle collisions. Note that while the Archimedes force term $V_p(\rho_p - \rho_1)$ is calculated with respect to the reference density ρ_1, the effect of local density changes on the particle motion are properly accounted by the IBM forcing, which appears implicitly in the stress tensor. In nondimensional form, the particle motion is given by

$$\frac{\rho_p}{\rho_1} \frac{d\mathbf{u}'_p}{dt'} = \frac{6}{\pi Re} \oint_{\Gamma_p} \tau'_h \cdot \mathbf{n} dA' - \frac{gD_p}{w_s^2} \left(\frac{\rho_p}{\rho_1} - 1 \right) \mathbf{k} + \mathbf{F}'_{c,p}, \tag{6a}$$

$$\frac{\rho_p}{\rho_1} \frac{d\omega'_p}{dt'} = \frac{60}{\pi Re} \oint_{\Gamma_p} \mathbf{r}' \times (\tau'_h \cdot \mathbf{n}) dA' + \mathbf{T}'_{c,p}. \tag{6b}$$

The model solved Eqs. (3) and (6) using second-order finite differences for spatial derivatives, an explicit third-order, low storage Runge-Kutta scheme for the convective terms, and a Crank–Nicolson scheme for the viscous terms. For each Runge-Kutta substep, the pressure was directly solved with fast Fourier transforms. The IBM was used to solve for the motion of the particles. Further details about the numerical model, especially the particulars of particle collisions, are presented in Biegert *et al.* [41] and Ouillon *et al.* [43].

For simplicity, the horizontal boundary conditions were periodic with a free slip condition used on the top and bottom boundaries. At the surface of the impermeable particles, the boundary condition for the velocity field was no-slip and no-flux, i.e., vanishing tangential and normal velocity components. The density field was prescribed with a no-flux boundary condition on on the particle, top, and bottom surfaces. Whereas the numerical model accounts for the momentum with the IBM, the density is accounted for through the volume-of-fluid method [44]. The smallest particle separation distance analyzed, $s_0/D_p = 1$, used a domain with dimensions $L_x \times L_y \times L_z = 12D_p \times 12D_p \times 30D_p$. To ensure that the side-wall boundaries did not significantly influence the particles, the simulation with horizontally aligned particles and weak stratification was repeated with double the horizontal dimensions. The particle settling speed in the wider case increased by approximately 10% compared to the narrow case. Although the wider domain had less resistance from the exchange of fluid moving upward as the particles settled, this had little impact on the particle-particle interaction, having a maximum difference in the particle separation of 3%. To minimize boundary effects, cases with larger initial separation distance used a domain width that was increased by the equivalent increase in particle separation. Cases with vertically aligned particles and large separation distance required a doubling of the domain depth so as to allow the particles sufficient distance to interact.

The lower particle was located three particle diameters above the center of the pycnocline ($h_p = 3D_p$). Simulations of an individual particle initialized at various h_p above the interface demonstrated that the behavior of the particles within the interface and lower layer were independent of the initial distance provided that $h_p > 3D_p$. In comparison, Blanchette and Shapiro [45] observed that a settling speed of 90% of the terminal velocity within the upper layer was indistinguishable within the lower layer from the settling of drops that were at their settling velocity when entering the interface. Although this was in the context of settling drops rather than particles, the agreement is supportive of our choice. More appropriately, the short distance was chosen to minimize

particle-particle interactions before reaching the interface. Similarly, the upper particle was initially located three particle diameters below the top of the domain ($h_T = 3D_p$). Sensitivity studies of values of h_T showed that distances shorter than $3D_p$ resulted in wall effects caused by the upper boundary. Minimal influence of the top boundary was found for distances larger than $3D_p$.

The rectangular domain was discretized with uniform grid cells of size $\Delta x = \Delta y = \Delta z = h$. The resolution of $h/D_p = 1/25$ was used for all cases reported upon here and is comparable to that for active rising or settling spherical swimmers [43] and sediment beds with relatively compact particle packing [41]. Grid refinement studies showed that the changes to the particle velocity was minimal (<5%) when the resolution was increased. Although the separation distance between the particles after coming in contact varied for different resolutions, this primarily occurred at strong stratification with vertically aligned particles for which the wake of the leading particle played a significant role.

III. RESULTS

The settling of a pair of particles for a variety of particle separations, orientation angles, stratification strengths, and Reynolds numbers is presented here. Before this, we first discuss the role of the stratification on the settling of a single particle and the interaction of a pair of particles in homogeneous fluid before investigating the more complicated settling occurring for a particle pair in a stratified fluid. Details on how the settling particles interact with each other and, more importantly, with the stratification by drawing upper layer fluid into the lower layer will be examined.

A. Single-particle settling

Here we investigate the flow associated with the settling of a single particle through the interface to understand the features of the wake and its potential influence on a trailing particle. The settling of a single particle in a stratified fluid has been examined previously through experiments and theory [20,21,26,27]. This is partially reviewed in Appendix A for the purpose of validating our numerical simulations. Consistent with this earlier work, our simulations showed that the settling of a particle through the interface led to a deformation of the interface as fluid from the upper layer remained attached near the particle (Fig. 2). Once in the lower layer, the wake of the particle contained upper layer fluid which, due to local buoyancy, created an updraft within a narrow column centered on the particle that was approximately $2D_p$ wide (vertical dashed lines in Fig. 2).

Comparison of this $2D_p$ wake width is made to the updraft, shown by the red contours in Fig. 2. The updraft was narrow in the stratified region for all stratification strengths $\Gamma > 0$ and decreased in height with increasing stratification strength due to the slower motion of the particle in the lower layer. In the context of a linearly stratified fluid, Hanazaki *et al.* [46] described the multiple instabilities within the wake. However, the Reynolds number of these instabilities were much greater than unity, well outside the range of applicability here. In all simulations analyzed herein, the wake remained coherent and did not break down. As a result of these features, the motion of trailing particles that are horizontally offset by more than two particle diameters are expected to be unaffected by the stratified wake of the leading particle.

For Stokes settling in an unstratified fluid, vertical symmetry is predicted for streamlines in the reference frame moving with the sphere [Fig. 2(a)]. As expected, the stratification broke the symmetry due to the attachment of upper layer fluid on the particle.

B. Particle-pair settling in a homogeneous fluid

Previous theoretical and experimental investigations into the dynamics of two particles settling at low Reynolds number have demonstrated that their collective settling speed is enhanced and experience a lateral drift if the particles are neither vertically nor horizontally aligned [33–38,47].

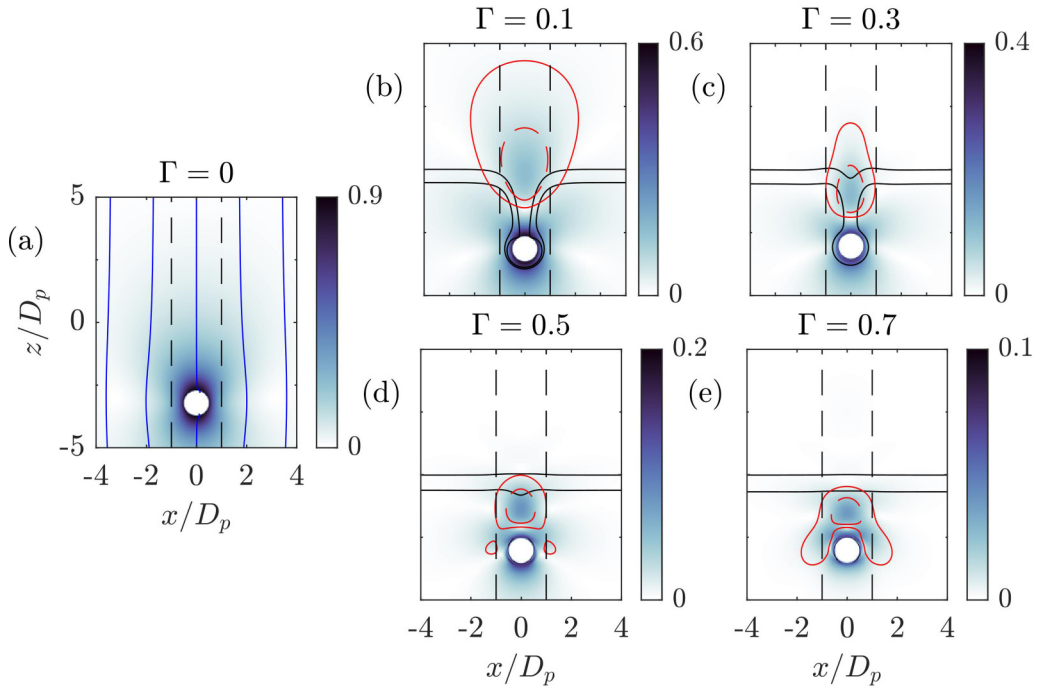

FIG. 2. Velocity magnitude cross section for a single particle when the particle was $3D_p$ below the interface. Solid contours are at $\rho' = 0.5$ and 0.75. Vertical dashed lines are at $x/D_p = \pm 1$. Note the differences in color scale between different subfigures. Blue streamlines are shown in (a) and red contours in (b)–(e) show where the vertical velocity is 10% (solid) and 50% (dashed) of the maximum upward velocity [there is no upward velocity in (a)].

Kynch [35] derived general formulas for the vertical, u_v, and horizontal, u_h, speeds of the particle pair centroid as

$$u_v/w_s = (K + \tilde{s}M) + (L + \tilde{s}N)\cos^2\theta, \tag{7a}$$

$$u_h/w_s = (L + \tilde{s}N)\sin\theta\cos\theta, \tag{7b}$$

where

$$\tilde{s} = \frac{D_p}{2(s + D_p)}$$

is the ratio of particle radius to the instantaneous distance between particle centres. Note that $\tilde{s}$ scales inversely with s, and the parameters K, L, M, and N in Eqs. (7) are high order polynomial fractions in $\tilde{s}$ presented in Appendix B.

Figure 3 plots the predicted (Stokes regime; solid lines) and simulated (Re = 1/4; markers) vertical and horizontal velocities of the centroid of the particles as they depend on orientation angle and separation. In the simulated cases, these velocities change over time because of inertia. To account for the varying relative particle positions, we choose the centroid velocities at $t = 3\tau$, which is enough to remove the transients of particle acceleration and short enough to limit the effects of relative particle motions.

Compared to Re = 0, increasing the Reynolds number to 1/4 has caused a reduction in the settling velocity of the pair but gives comparable horizontal drift. Independent of inertia, the maximum vertical speed occurred when the particles were vertically aligned and were close together. Increasing the orientation angle led to a monotonic decrease in the vertical velocity. Equation 7(b)

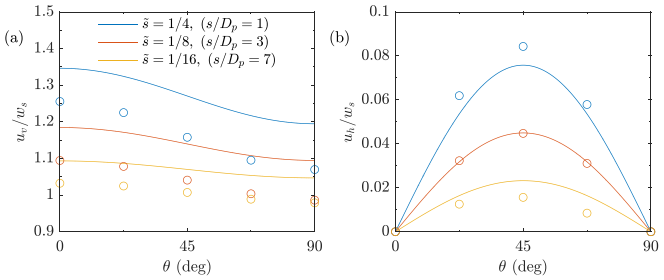

FIG. 3. (a) Vertical and (b) horizontal speeds of a pair of particles in a homogeneous fluid as given by Eq. (7) (solid lines) and for Re $= 1/4$ (markers). The Re $= 1/4$ cases are compared against the settling velocity of an individual particle with Re $= 1/4$.

predicts that the maximum horizontal drift occurs when the particles are at an angle of 45° and no lateral drift when the particles are vertically or horizontally aligned ($\theta = 0, 90°$, respectively) [Fig. 3(b)]. Even without the presence of stratification, the motion of a particle pair is highly dependent on their relative positions.

Although the theory just presented is for Re $= 0$, a consistent use of simulations with Re $= 1/4$ are presented in the results that follow, where we will demonstrate that the presence of a density interface temporarily alters the speed and orientation of the particle pair. Later, in Sec. III G, it will be shown that the influence of inertia is reduced in the presence of stratification.

C. Particle-pair settling in a stratified fluid: Qualitative results

In a homogeneous fluid, two particles interacted with each other as they settled, thereby changing their vertical, and possibly horizontal, speeds of descent. With the introduction of a stratified interface, the particles deformed the interface as they approached and subsequently passed through it. Consequently, the particles decelerated due to the deformation as well as the change in buoyancy force acting on the particles within the lower layer.

The deformation of the density field due to the particle pair settling was evident when the particles passed through the interface at nondimensionalized time, $t/\tau = 6$, as shown in Figs. 4(a)–4(c). A large deformation of the interface occurred when the stratification was weak [$\Gamma = 0.1$ for Figs. 4(a) and 4(b)] compared to the stronger stratification ($\Gamma = 0.5$) in Fig. 4(c). Later, once the particles fell within the lower layer [Figs. 4(d)–4(f)], the interface returned to its equilibrium position except for a trail of upper layer fluid within the wake of the particles. Some of this fluid was carried by the particles to depth.

As in the case of a homogeneous fluid, when the particles were neither vertically nor horizontally aligned [i.e., $\theta \neq 0, 90°$, Figs. 4(b), 4(c) 4(e), and 4(f)], the pair experienced a horizontal drift due to the interaction of the trailing particle with the wake of the leading particle. Although the drift is due to the relative positions of the particles, we will show that the stratification influences the settling and drift rate as well as the orientation angle between the particles. Figures 4(b) and 4(e) shows a case with the particles at an initial orientation angle of $\theta = 67.5°$. Both particles drifted to the right, as determined by the location of the leading particle relative to the trailing particle. When the orientation was the same but the stratification was stronger [Figs. 4(c) and 4(f)], particles spent more time passing through the interface and settled more slowly in the lower layer, with their orientation being more horizontal than when they started.

D. Particle-pair orientation, drift, and settling speed

The previous two sections have revealed that the settling behavior of a particle pair is dependent on the orientation of the particles. Most notably, the lateral drift depends on the orientation and the settling speed depends on the particle separation.

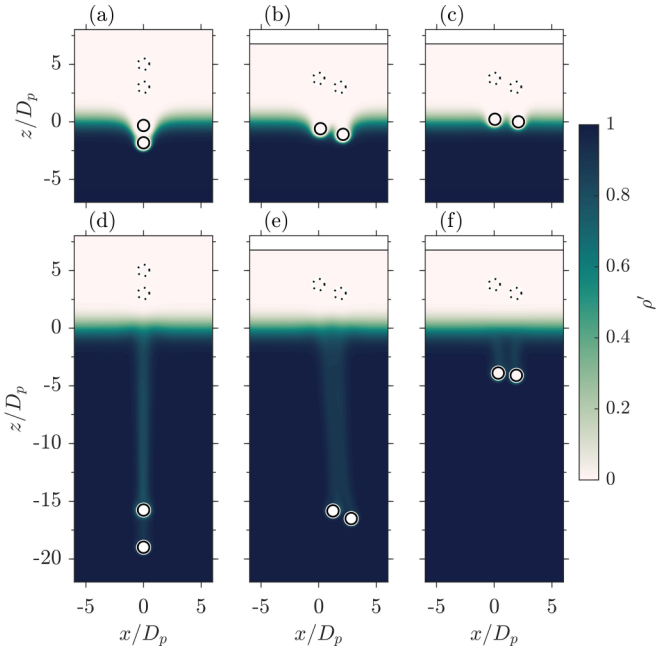

FIG. 4. (Supplemental Material online [48].) Snapshots of the nondimensional density field and particle positions for (a), (d) $\Gamma = 0.1$ and $\theta = 0°$; (b), (e) $\Gamma = 0.1$ and $\theta = 67.5°$; and (c), (f) $\Gamma = 0.5$ and $\theta = 67.5°$. The upper and lower rows are at $t/\tau = 6$ and $t/\tau = 30$, respectively. The particles were initially $s_0/D_p = 1$ apart and are shown as the upper two dotted circles.

The instantaneous orientation angle for the settling pair for various initial orientation angles and stratification strengths is shown in Fig. 5. When settling in a homogeneous fluid (black lines), the simulations show that the angle increased with time due to the fluid inertia. When passing through a stratified interface, the leading particle decelerated earlier than the trailing particle causing the orientation angle to increase when the particles were initially neither vertically nor horizontally aligned. That is, the particles became more horizontal as the trailing particle caught up to the leading one (Fig. 5). This increase in orientation angle was temporary for weak and moderate stratification ($0 < \Gamma < 0.5$) before inertia began to increase the orientation angle with the release of the attached upper layer fluid from the particles. However, if the stratification was very strong ($\Gamma = 0.7$, purple

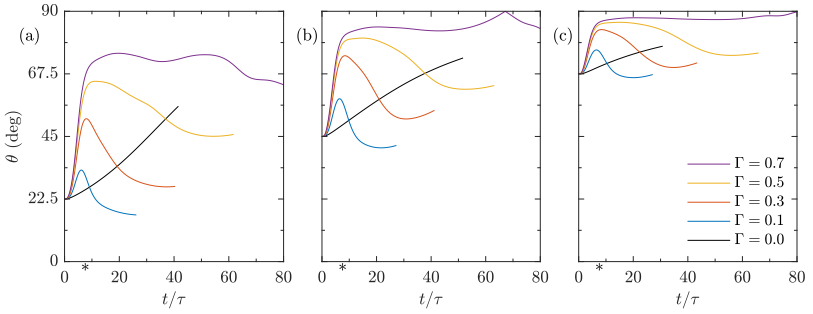

FIG. 5. Orientation angle versus time as it depends on stratification for $s_0/D_p = 1$ and (a) $\theta = 22.5°$, (b) $\theta = 45°$, and (c) $\theta = 67.5°$. The particles passed through the interface at approximately $t/\tau = 6$ ($*$ on horizontal axis).

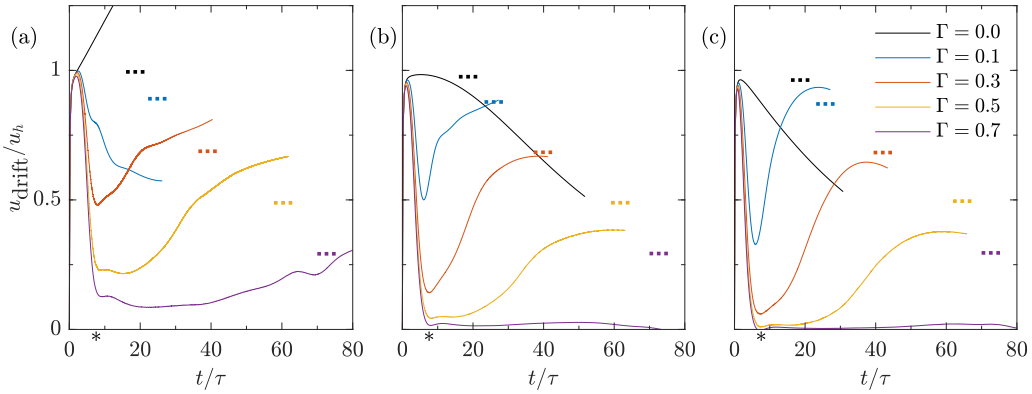

FIG. 6. Horizontal drift velocity versus time as it depends on stratification for $s_0/D_p = 1$ and (a) $\theta = 22.5^\circ$, (b) $\theta = 45^\circ$, and (c) $\theta = 67.5^\circ$. The horizontal drift is scaled by the upper layer drift velocity as predicted by Eq. (7b). The thick, dashed horizontal lines are the lower layer horizontal drift speeds for $\text{Re} = 1/4$ once the particles have accelerated from rest. The particles passed through the interface at approximately $t/\tau = 6$ ($*$ on horizontal axis).

line), the orientation angle remained large over the simulations. In the $\theta = 45^\circ$ and $\theta = 67.5^\circ$ cases, the trailing particle even caught up to the leading particle and surpassed it.

As the leading particle passed through the interface, the interface deflected in such a way to temporarily form a potential well. However, the trailing particle was not drawn into this well as this would have caused the orientation angle to transition to low values. This is evident in Fig. 5 for $\theta = 45^\circ$, which shows the orientation angle increasing, as was the case for particles oriented at other angles (see also the Supplemental Material [48]). Figure 4(b) shows that the trailing particle has not shifted laterally behind the leading particle (see also Supplemental Material). Rather, possible attraction by the potential well was counteracted by the upward return flow within the wake of the leading particle (where this updraft was discussed for a single particle in Sec. III A.

Both the variation in orientation angle and the hindered settling speed as the particles passed through the interface was partially responsible for the variations in the drift speed of the particles. Figure 6 shows the horizontal drift speed, u_{drift}, relative to the predicted upper layer drift speed, u_h, based on the initial particle separation and angle as given by Kynch [35]. After the initial acceleration phase the homogeneous fluid case ($\Gamma = 0$) was close to the expected drift speed, but deviated over time due to inertia (as also seen in the orientation angle, Fig. 5). When passing through the stratified interface, the normalized drift speed decreased because of the hindered settling. In the case of $\theta = 45^\circ$ and 67.5°, the drift speed may also be reduced because the particles became more horizontally aligned. When $\theta = 22.5^\circ$ the trailing particle is within the $2D_p$ diameter wake of the leading particle which causes its settling to be modified by the upper layer fluid within the wake of the leading particle.

Comparison of the drift in the lower layer is made to that of two inertial particles initialized within a homogeneous fluid of density matching that of the lower layer (thick dashed lines). The representative quantity for the drift speed is taken at $t/\tau = 2$ when the particles have accelerated but have had little influence due to inertia. Qualitatively, the trends in the observed drift speeds due to the stratification agree with the observed values for $\theta = 45^\circ$ and 67.5° with moderate and low stratification strengths after the majority of upper layer fluid surrounding the particles was drawn back to the upper layer. Despite clear discrepancies in the predicted and observed lower layer drift speed due to the particle separation and orientation angles changing when passing through the interface, the drift speed qualitatively agrees with the low Reynolds number theory within the lower layer when the stratification was not too strong. The strong stratification case ($\Gamma = 0.7$) had a very slow drift velocity due to the particles becoming effectively horizontal (see Fig. 5).

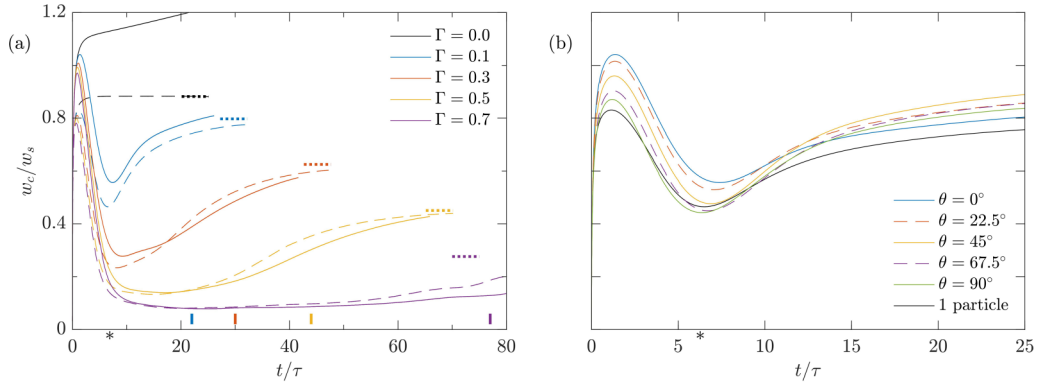

FIG. 7. Vertical settling speed of the particle pair centroid versus time as it depends upon (a) stratification with $\theta = 0^\circ$ (vertically aligned particles) and (b) orientation angle for $\Gamma = 0.1$ (a weak stratification). The thick, dashed horizontal lines are settling velocities for a single particle within the lower layer at $\mathrm{Re} = 1/4$ once the particle has accelerated from rest. All cases had $s_0/D_p = 1$. The particles passed through the interface at approximately $t/\tau = 6$ ($*$ on horizontal axis).

The influence of the stratification on the vertical settling speed of the centroid of a pair of particles as determined from numerical simulations is shown in Fig. 7. In a homogeneous fluid, the pair of particles (solid black line) rapidly accelerated from rest to speeds greater than the Stokes settling speed of a single particle. The enhanced speed of two particles collectively settling is due to the mutual interaction of the particle wakes leading to a reduction in drag [35]. The settling of the single particle (dashed black line) is slower than the predicted value because of increased drag due to self-interaction through the narrow periodic side walls and inertial effects. Further exploration of the role of inertia will be made in Sec. III G.

When the stratification was present, the particles passed through the interface at $t/\tau \approx 6$, causing the particle descent to slow dramatically. In part, this was because the buoyancy of the particles relative to the lower layer density was reduced but also because the particles carried upper layer fluid along with them, making them more positively buoyant relative to the surrounding ambient fluid. For the strongest stratification considered ($\Gamma = 0.7$), the particle settling speed was reduced by approximately 90% when passing through the interface. Even in the weak stratification case with $\Gamma = 0.1$ there was a dramatic reduction in the settling speed by approximately 50%.

Once in the lower layer, the settling speed of the particle pair increased toward the settling rate of a single particle [short horizontal lines in Fig. 7(a)] as a result of the gradual release of the upper layer fluid surrounding the particles. The occurrence of a minimum settling speed as the particles passed through the interface is in agreement with many previous studies of a single particle settling through an interface [20,22,23,49]. Verso *et al.* [23] found that the timescale for a particle to release the surrounding upper layer fluid after passing through a salt stratified interface was proportional to D_p/w_2, where w_2 is the measured settling speed in the lower layer. Although Verso *et al.* [23] investigated particles at moderate Reynolds numbers for which $w_2 \not\approx w_{s,2}$, this approximation is valid from our observations. Using this approximation and scaling by our characteristic time τ, the recovery timescale is $13 w_s/w_{s,2} = 13\rho_2/[\rho_1(1-\Gamma)]$. The stratifications in Fig. 7(a) have normalized recovery times of 16, 24, 38, and 71 for $\Gamma = 0.1$, 0.3, 0.5, and 0.7, respectively. Even though the recovery time from Verso *et al.* [23] was developed for a single particle, because the settling of the particle pair mimicked that of a single particle this estimate should be suitable. Shown as thick vertical colored lines in Fig. 7(a), the predicted recovery times increase with the stratification strength.

In comparison to the settling of a single particle [dashed lines in Fig. 7(a)], the pair of particles initially had a faster settling rate within the upper layer. In most of the stratified cases, the settling

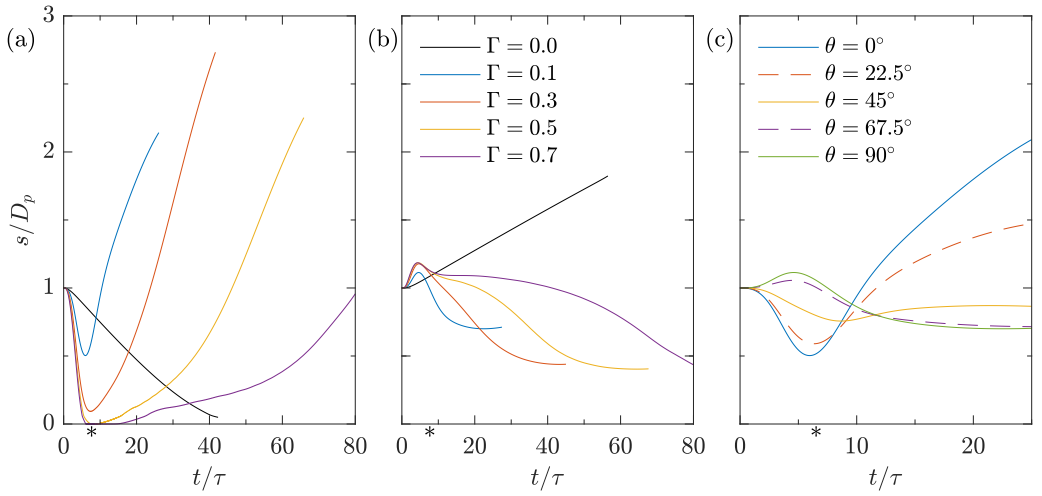

FIG. 8. Particle separation versus time as it depends on (a) stratification for $\theta = 0°$, (b) stratification for $\theta = 90°$, and (c) orientation angle for $\Gamma = 0.1$. All cases had $s_0/D_p = 1$. The particles passed through the interface at approximately $t/\tau = 6$ ($*$ on horizontal axis).

rate for the particle pair in the lower layer remained slower than that of the single particle (dashed line). This difference was due to a time delay arising in the duration for the trailing particle to pass through the interface. This delay was not present when the particles settled side by side (not shown), in which case the particle pair reached a faster settling speed in the lower layer when compared to that of a single particle. The weak stratification case with $\Gamma = 0.1$ did not fit this description of the delay because the particles passed through the interface relatively quickly.

The orientation angle, θ, of the particles had only a minor influence on the particle-pair settling speed [Fig. 7(b)]. The maximum initial settling speed occurred when the particles were vertically aligned and decreased with increasing angle, again consistent with theory. Once the particles were in the lower layer, the release of upper layer fluid from the leading particle hindered the settling speed of the trailing particle, marginally more for vertically aligned particles. When compared to the changes seen in the settling speed due to the stratification, the orientation angle is less impactful. Although the particle settling is affected by a variety of factors (such as the domain size, resolution, Reynolds number, and the IBM method), the dependence on the stratification strength remains robust for the fixed conditions used within the simulations.

E. Particle-pair separation

The particle separation distance, s, gives an indication of how the particle interactions can strengthen or weaken, especially if they come into contact with each other. Particles that come into contact may combine into a single, larger particle, for example if they are electrically charged or chemically reactive. Consolidated particles would likely exhibit enhanced settling due to their larger effective size. Within the IBM particle model and with the resolution typically used for the simulations, the particles can be considered to be touching if $s/D_p < 0.05$.

Observations and theory on the settling of two particles in a homogeneous fluid have shown that two particles will approach when settling vertically but separate when settling horizontally for the Reynolds number considered here [47]. Our numerical simulations agree with this prediction [Figs. 8(a) and 8(b)].

For vertically aligned particles [Fig. 8(a)], stratification caused the particles to rapidly approach each other when passing through the interface, coming into contact if the stratification was sufficiently strong ($\Gamma \gtrapprox 0.5$). Because no cohesion model was used in our simulations, the particles

then began to separate within the lower layer as the trailing particle experienced additional drag due to the upper layer fluid draining upwards from the leading particle. The particles separated earlier because they more rapidly passed through the interface when the stratification was weak, which then caused the drainage of upper layer fluid to occur sooner. Our simulations were unable to identify if the particles eventually separated in the case of a homogenous fluid because this would have required a large domain depth. However, they do reveal that the particles converged at a considerably slower pace in a homogenous fluid than in simulations with a density interface. Weak stratification prevented the contact of the particles, unlike the homogenous cases for which the particles collided.

When the particles were side by side [Fig. 8(b)], they initially increased in separation as they approached the interface as expected within a homogeneous fluid. However, once in the lower layer the trailing stratified particle wakes caused the particles to draw closer together before reaching a minimum separation distance. Doostmohammadi and Ardekani [39] argued that the stratification formed a vertical jet which induced a horizontal convergence zone between the particles. Because the stratification was temporary, the jet and convergence zone eventually weakened, thereby ending the particle attraction. The simulations showed that particle separation in the lower layer began once the majority of the upper layer fluid was detached. Unlike the case of vertically aligned particles that simultaneously reached their minimum separation when passing through the interface, horizontally aligned particles reached their minimum separation at a time that increased with stratification strength.

The separation distance for a variety of orientation angles with $\Gamma = 0.1$ [Fig. 8(c)] shows the importance of the initial orientation angle upon the relative motion of the particles as they passed through the interface. Approximately horizontally aligned particles initially separated from each other before passing through the interface but remained relatively close within the lower layer. This is in contrast to particles that were initially vertically aligned. These at first approached each other when passing through the interface before rapidly separating. Particles initially at $\theta = 45^\circ$ began, at first, to behave as vertically aligned particles by becoming closer, but later acted as horizontally aligned particles by remaining relatively close. Comparing the particle-pair settling within a linearly stratified fluid [39] to the two limiting cases herein (horizontal and vertical particle alignment) shows qualitative agreement; vertically aligned particles approach before separating rapidly, whereas horizontally aligned particles remained close for the duration of the simulation.

We highlight that the orientation angle plays a more important role in the separation distance when compared to the role it had on the vertical settling velocity of the particle pair. The significant differences between the vertical and horizontally aligned particles is accounted for by the wake flow of a single particle discussed in Sec. III A and its implications on the trailing particle in Sec. III D. The vertical updraft interacted with the trailing particle causing the particles to separate when in vertical alignment. At large orientation angles ($\theta > 45^\circ$), when the trailing particle did not interact with the leading particle wake, the particle separation dynamics were similar.

The minimum separation distance for a large suite of stratifications, particle separation, and particle orientations is shown in Fig. 9. As seen in Fig. 8, the particles did not come closer than half their initial separation distance in weak stratification ($\Gamma = 0.1$) for any orientation angle. In general, the particles' minimum separation distance increased with initial orientation angle for a fixed stratification.

The particles were found to reach smaller minimum separation distances with increasing stratification. This agrees with the notion that a strong stratification rapidly decelerates the leading particle while the trailing one continues to approach from above. At high orientation angles (horizontal alignment), the particles approached but did not come in contact.

On a relative scale, the minimum particle separation for a fixed orientation angle was effectively independent of the initial separation distance [Fig. 9(b)]. In agreement with what has been shown thus far, the particles reached smaller separation distances when the particles were more vertically aligned as opposed to horizontal. In fact, horizontally aligned particles that were spaced more than two particle diameters apart showed negligible attraction for this weak stratification.

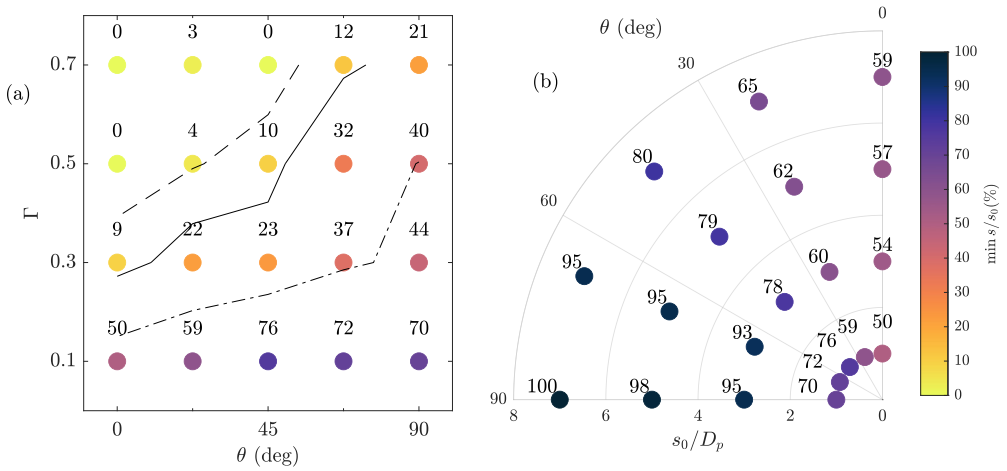

FIG. 9. Minimum relative particle separation, $\min s/s_0 \times 100\%$, as it depends on (a) stratification and particle orientation for $s_0/D_p = 1$ and (b) initial particle separation and orientation for $\Gamma = 0.1$. In (a), the dashed, solid, and dashed-dotted contour lines correspond to $\min s/s_0 = 5\%$, 15%, and 40%, respectively.

F. Fluid entrainment

Of interest to us is whether there is an increase or decrease in entrained fluid when two interacting particles are settling as compared to the entrainment of two well-separated particles. Should there be an increase, even marginally, this effect would be amplified for a large number of particles, possibly even at low concentration. In this case, particle clouds could play a significant role in mixing interfaces [12,50] and drawing fluid from the surface to depth (or from depth to the surface in the case of buoyant particles or bubbles [51,52]). In the context of the motion of a single particle in a linearly stratified fluid Inman *et al.* [26] found simple scaling laws for the maximum displacement of an isopycnal.

The entrainment is defined from a continuous passive tracer field initialized similarly to the background density profile:

$$c(z) = \tfrac{1}{2}[1 + \mathrm{erf}(z/\sigma)].$$

Here, $c = 1$ well within the upper layer and 0 well within the lower layer. The evolution of this tracer field is equivalent to Eq. 2(c) where the diffusivity of the tracer field was the same as that of the density field. Although the density field could be utilized in this formulation when stratification is present, it would be meaningless when the fluid is homogenous. Rather, we conceptualize the entrainment with a passive tracer as would be the case of dye within a laboratory experiment.

The particles, which were situated initially at rest within this tracer field, were found partially to transport the tracer downward as they settled, in a similar way to what is seen in Fig. 4. We define the instantaneous entrainment as the deviation of the tracer field from the background

$$C_{\mathrm{entrain}} = \int (c - \bar{c})\phi_f dV, \tag{8}$$

where $\bar{c}(z,t)$ is the time-evolving background tracer profile (as caused by diffusion rather than the particle motion) and ϕ_f is the volume fraction of fluid (0 inside particle and 1 outside).

As the particles approached the interface, the instantaneous entrainment increased due to the deformation of the interface they induced [Fig. 10(a)]. As seen in Secs. III A and III C, once the particles passed through the interface the captured fluid surrounding each particle began to separate from the particle resulting in a trail of upper layer fluid returning upwards within the lower layer.

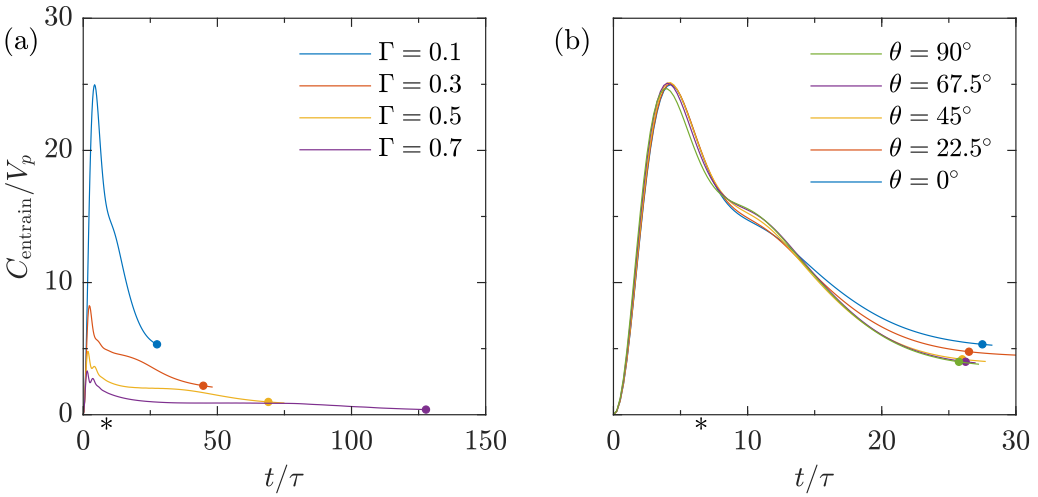

FIG. 10. Entrainment versus time for different (a) stratification with $\theta = 0$ and (b) orientation angle for $\Gamma = 0.1$ and $s_0/D_p = 1$. Solid markers represent the time when the trailing particle is 15 particle diameters below the center of the interface.

This fluid, which contained the tracer field, in part slowly returned to its depth of neutral buoyancy, causing the reduction of C_{entrain}.

Unsurprisingly, increasing stratification led to a reduction in the amount of entrainment because the particles moved slower and greater conversion from kinetic to potential energy was needed to transport fluid through the interface. At $t/\tau = 30$, the homogeneous fluid case had $C_{\text{entrain}}/V_p = 195$. In comparison, the case with $\Gamma = 0.1$ at the same time had $C_{\text{entrain}}/V_p \sim 5$; approximately a 40-fold decrease. Figure 10(b) makes it clear that the entrainment was largely independent of orientation angle for the weak stratification and initially close particles. Only at late times did the entrainment increase slightly for the vertically aligned cases, in which the trailing particle recaptured some of the lost tracer from the leading particle. If the orientation angle was such that the trailing particle did not interact with the tail of the leading particle ($\theta \gtrapprox 22.5°$ for $s_0/D_p = 1$), the entrainment was independent of orientation angle.

More important than the temporal evolution of the entrainment is the final value of entrainment. This provides an estimate of the efficiency of transport of upper layer fluid to depth. We define the final state as when the trailing particle was 15 D_p below the center of the interface. This distance was found to remove many of the transients of the interface deformation from the passage of the particles through the interface.

The final relative entrainment as a function of the stratification and particle orientation for $s_0/D_p = 1$ is presented in Fig. 11(a). This compares the entrainment of an interacting particle pair with two noninteracting particles. The largest enhancement of entrainment occurred at low orientation angle and weak stratification. For $\Gamma = 0.1$ and $\theta = 0°$, the entrainment of the particle pair was 40% greater than two individual particles on their own. However, most cases with strong stratification and large orientation angle showed only weak, if any, enhancement of entrainment.

The lack of enhanced entrainment is especially evident when comparing the entrainment for various initial separation distances and orientation angles for $\Gamma = 0.1$ [Fig. 11(b)]. For the majority of angles and relative particle separations, the collective settling had negligible impact on the entrainment unless the particles were vertically aligned or were initially close together. Section III A showed that the wake of the leading particle was two particle diameters wide. Recast in terms of the initial particle separation the wake edge was at $s_0/D_p = 0.5$ (black line in Fig. 11). It is evident that

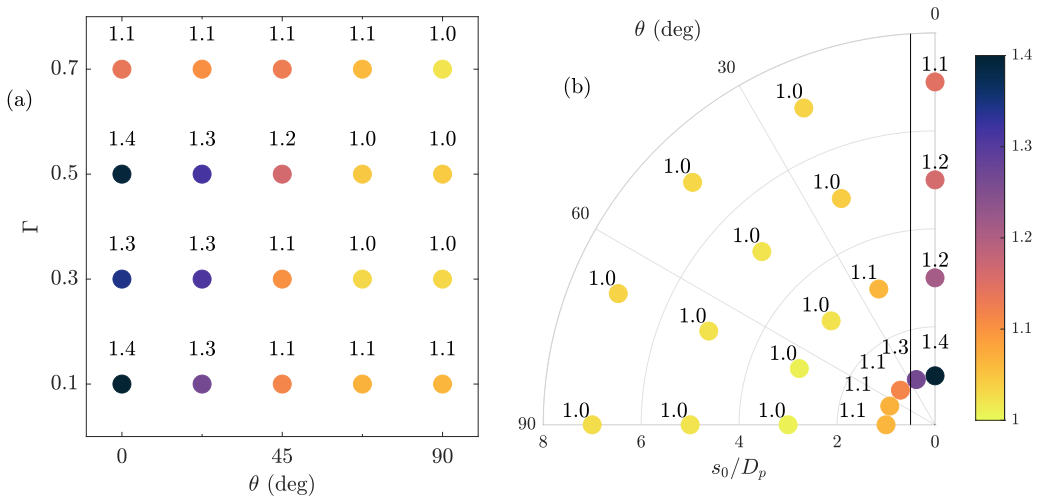

FIG. 11. Final entrainment relative to two noninteracting particles as a function of (a) stratification and particle orientation for $s_0/D_p = 1$ and (b) initial particle separation and orientation for $\Gamma = 0.1$. The vertical black line in (b) represents the edge of the wake of the leading particle.

the trailing particle substantially enhanced entrainment only when trailing within the wake of the leading particle.

Comparing the dependence of final entrainment on the stratification, orientation angle, and separation distance to that of the minimum particle separation distance (Fig. 9) shows that there is no correlation between the minimum separation distance and the value of fluid entrainment. At least with regard to two particles, the entrainment is independent of how near the particles become. The only important factor for entrainment is whether the trailing particle is within a narrow column (two particle diameters wide) above the leading particle corresponding to the wake of that particle as shown in Fig. 2.

G. Role of fluid inertia

To reduce numerical costs, the results presented so far set $\mathrm{Re} = 1/4$, which is approximately four times larger than the upper bound for Stokes regime. In Fig. 7(a), the settling speed of the single particle in the homogenous fluid ($\Gamma = 0$, dashed black curve) was slower than the Stokes settling speed by at approximately 13% because of the relatively large Reynolds number. Furthermore, in violation of the theory on particle pairs in Stokes flow, the settling speed of the pair in the homogenous fluid continued to increase over time [33,35,36]. Further inertial effects are evident in the homogeneous fluid cases of Figs. 8 and 5, where the particles' relative distances and orientations change over time. From these observations, it is clear that inertia was non-negligible when settling in a homogeneous fluid. It is then natural to ask if inertia was an important factor when the fluid was stratified for the present choice of Reynolds number.

The relative importance of the stratification to inertial forces is quantified by the Richardson number,

$$\mathrm{Ri} = \mathrm{Fr}^{-2} = \frac{g\Delta\rho D_p}{\rho_1 w_s^2}. \tag{9}$$

From the definition of the Reynolds number, the Stokes settling velocity and Γ, this can be simplified to

$$\mathrm{Ri} = 18\frac{\Gamma}{\mathrm{Re}}. \tag{10}$$

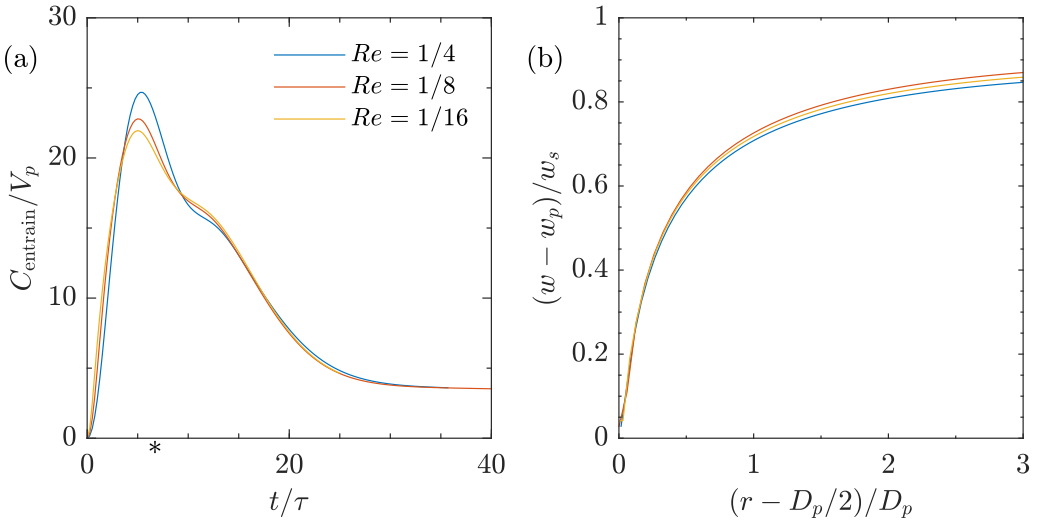

FIG. 12. (a) Entrainment and (b) vertical velocity near the sphere for various Reynolds number for initially close, horizontally aligned particles in weak stratification ($s_0/D_p = 1$, $\theta = 90$, and $\Gamma = 0.1$). w_p is the measured settling velocity of the particle and r is the distance along a horizontal radial direction from the center of the rightmost particle.

In this way, viscous forces dominate inertial ones when the Reynolds number is small ($\text{Re} \lessapprox 0.1$). However, stratification dominates inertial *and* viscous forces for even moderate values of $\Gamma > 0.014$ if $\text{Re} = 1/4$. As such, the role of inertia is not expected to be significant during the passage of the particles through the interface or while the particles carried upper layer fluid into the lower layer. Modeling [23] and experiments [20,21] show that the surrounding upper layer fluid separates from the particles after a finite time within the lower layer, at which point inertia will no longer be negligible due to the loss of stratification. Nevertheless, the stratification likely played a greater role than inertia in the entrainment because this occurred while the particles passed through the stratified region.

Two additional simulations were performed with Reynolds numbers less than 1/4 to investigate the sensitivity to Reynolds number when stratification was present. Figure 12(a) shows the time evolution of entrained fluid in three simulations with weak stratification ($\Gamma = 0.1$) and with $\text{Re} = 1/4$, 1/8, and 1/16. Before reaching the interface, the particles were inertially dominant which resulted in differences in the early entrainment. However, minimal difference in the entrainment was found once the particles were well into the lower layer. This suggests that the final entrainment value is adequately approximated with the use of $\text{Re} = 1/4$.

To ensure proper comparison between these cases of different Reynolds number, we maintained the same Schmidt number. With this in mind, the density boundary layer thickness remained largely unchanged between these simulations. The observed viscous boundary layer thickness, as evident from the vertical velocity near the rightmost particle, demonstrates that the viscous boundary layer was essentially the same for all cases [Fig. 12(b)].

IV. DISCUSSION AND CONCLUSIONS

Many experiments and simulations have previously been performed to examine particle pair settling in homogenous and stratified fluids [32,37–39,53]. However, they have by and large been concerned with particles that are in either vertical or horizontal alignment. Particles are rarely ever in these configurations nor do they remain in them for long. Thus our description fills a gap in our understanding of how particles pairs behave in a stratified environment; namely that particles in

approximate vertical alignment interact through the influence of the deformed density field, while particles offset laterally behave more independently of each other.

We have presented numerical simulations of a pair of particles settling through a thin interface with an aim to understand the relevant parameters for entrainment of upper layer fluid into the lower layer. When compared to two independently settling particles, we have shown that fluid entrainment increased when the particles are approximately vertically aligned due to the trailing particle re-entraining fluid from the wake of the leading particle. However, when the trailing particle was laterally offset by more than two particle diameters, the entrainment was the same as that of two independently settling particles. The fluid entrainment was strongest at weak stratification for which a greater volume of upper layer fluid was drawn into the lower layer.

Our ultimate goal is to make inferences about the particle-particle interactions and fluid collective transport by a large number of particles, especially with regard to how significantly interstitial fluid could be carried by the settling particles even at low particle concentration [10]. In designing this study of particle pair settling, we hypothesized that the leading particle would deform the interface such that the trailing particle would be drawn into the wake of the leading particle, thereby increasing the effective size of the settling particle and increase the volume of entrained fluid. However, our results do not support this notion. Rather, the returning upward draft within the wake of the leading particle is a horizontally divergent flow which effectively pushes the trailing particle laterally away. Thus, the original question regarding how significantly interstitial fluid is carried by a large cluster of particles remains an open problem. It is likely that the presence of a significant number of particles changes the bulk properties of the settling behavior. Alternatively, the enhanced fluid entrainment could be a product of how the settling plume formed. In the experiments of Sutherland *et al.* [10], the settling particle plumes formed in the presence of shear along the boundary between a gravity current and the underlying ambient fluid. Each individual plume might then have a greater average density than the lower layer, and thereby settle as a single entity. The background conditions for the plume formation likely plays a significant role in how much interstitial fluid may be entrained by the particles as they settle.

The complicated settling dynamics of multiple particles in a homogeneous fluid were discussed in a brief article by Slack [54]. The author observed that there are two regimes of collective particle settling: (1) coherent settling dynamics for particle clusters containing fewer than eight particles and (2) chaotic particle settling for clusters with greater than eight particles. From this, it is inferred that the complexity of the settling dynamics greatly increases with the addition of even a moderate number of particles. Including the effect of stratification on the settling dynamics, as we have done, only enhances the complexity. It is, then, difficult to make applicable extrapolations of the settling of a small number of particles on the behavior of many.

Although we did not concern ourselves with cohesion dynamics when particles came in contact, it is expected that many particles within the low Reynolds number regime considered here will remain as a single aggregate when they collide. Particle collisions occurred in strong stratification and low particle orientation angle. For a turbulent background, the particle dynamics are more complicated, but generally act to increase the likelihood that particles can come in contact and possibly aggregate. It is well known in the marine biology literature that the settling of organic matter interacts to form large aggregates which are hindered when settling through density interfaces [2]. In the ocean, MacIntyre *et al.* [2] observed particles settling with Reynolds number in the range 0.2–23 and Froude number between 5 and 70. Equation (9) then reveals Γ in the range 2×10^{-4} to 0.05. Although this is small, the hindered settling of the observations align with the results shown here.

Although we have considered a relatively thin interface, the influence of the interfacial thickness will be nontrivial on a pair of settling particles. If passing through a very thick interface relative to the particle size, the environment could be comparable to a linear stratification. Particles settling through this environment continuously enter layers of successively denser fluid, which adjusts the drag force on the particles [27,39,55]. Although the form of the stratification may change, the width of the trailing wake is not expected to be significantly different. Thus, a trailing particle would be

influenced by the leading particle only if situated within the approximately two particle diameter wide wake behind the leading particle. Ongoing work is testing these hypotheses in the context of multiple settling particles.

ACKNOWLEDGMENTS

This research was, in part, supported by Natural Sciences and Engineering Research Council of Canada (NSERC) Discovery Grant No. RGPIN-2015-04758. Simulations were completed on Compute Canada's high performance computing clusters Graham and Cedar. D.D. is grateful to K. Zhao at UCSB for the support he gave regarding implementation of the numerical model.

APPENDIX A: SINGLE PARTICLE VERIFICATION

The numerical model used herein was validated by comparing the settling of particles against previous laboratory experiments and numerical simulations in various configurations and stratifications.

Mordant and Pinton [56] accurately measured the settling of a single sphere in a homogenous fluid using acoustic transducers for a wide range of Reynolds numbers. We compared against the case with the smallest Reynolds number, $\mathrm{Re} = w_{\max} D_p/\nu = 41$ for a particle with density $\rho_p/\rho_0 = 2.56$. The model domain size was $20D_p \times 20D_p \times 30D_p$ with a resolution of $\Delta x = 1/20D_p$. Good agreement between the particle settling time series was found for the duration of the simulation [Fig. 13(a)].

Ten Cate *et al.* [57] measured particle settling at lower Reynolds numbers and particle density than Mordant and Pinton [56]. These values are more suitable for the conditions considered here. The Reynolds number and particle density were $\mathrm{Re} = w_{\max} D_p/\nu = 1.5$ and $\rho_p/\rho_0 = 1.155$, respectively. The domain size ($7D_p \times 7D_p \times 11D_p$) was chosen to be close that used in the experiment.

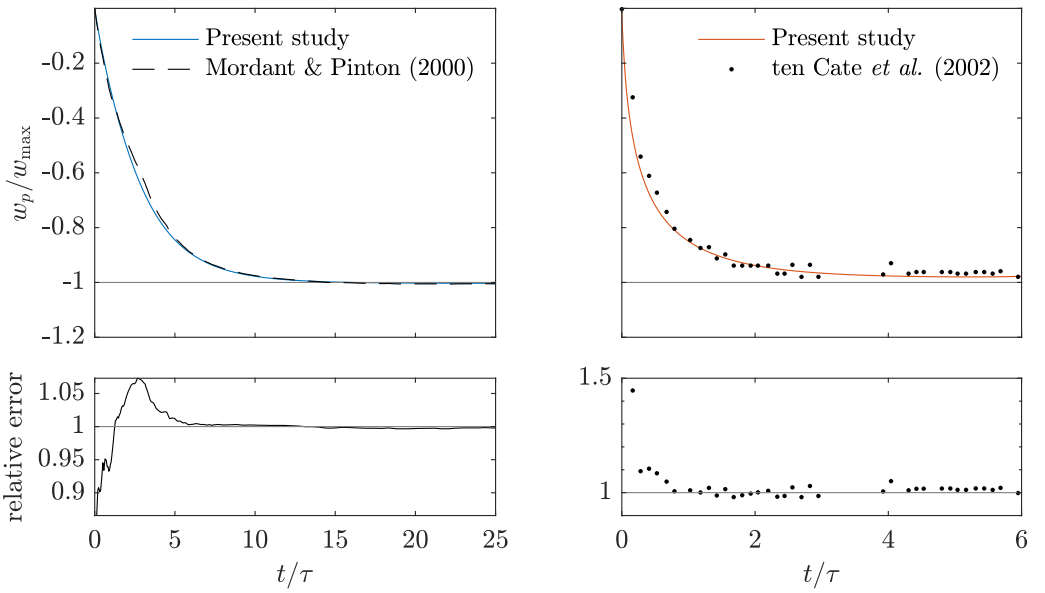

FIG. 13. Experimental comparison of the settling of a sphere in a homogenous fluid with a) $\mathrm{Re} = w_{\max} D_p/\nu = 41$ and $\rho_p/\rho_0 = 2.56$ (Mordant and Pinton [56]) and b) $\mathrm{Re} = w_{\max} D_p/\nu = 1.5$ and $\rho_p/\rho_0 = 1.155$ (ten Cate *et al.* [57]).

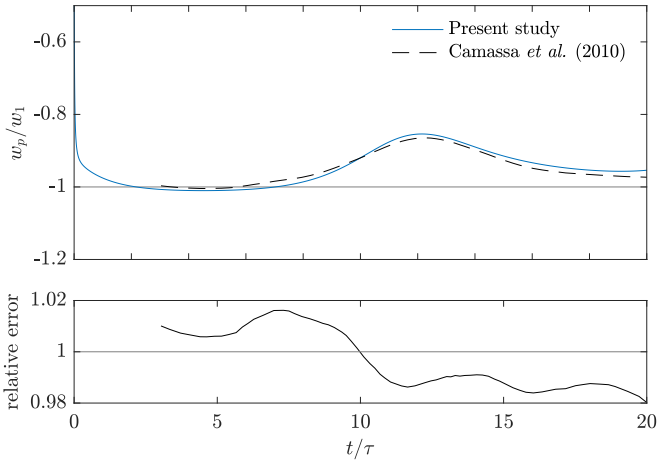

FIG. 14. Particle settling velocity through a thin interface between two fluid densities.

The resolution was $\Delta x = 1/30D_p$. The time series of the settling particle again matches well with our model results [Fig. 13(b)].

More appropriate for the present research is the study of Camassa *et al.* [21] who measured the settling of a single sphere through a sharp interface at a low Reynolds number, $Re = w_1 D_p/\nu = 0.0373$, where w_1 is the observed settling velocity in the upper layer. The particle density was $\rho_p/\rho_1 = 1.0654$ and the interface had a half-width of $0.3D_p$. The stratification was weak at $\Gamma = 0.0166$. The domain and resolution were $12D_p \times 12D_p \times 25D_p$, and $\Delta x = 1/20D_p$, respectively. Given that the thickness of the interface in the simulation was thicker than that in the experiment, the agreement for the settling velocity is quite good (Fig. 14).

Data from previous works has been extracted from the associated papers via the online WEBPLOTDIGITIZER tool [58].

APPENDIX B: COEFFICIENTS OF PARTICLE VELOCITIES IN A HOMOGENEOUS FLUID

The coefficients of Eq. (7), the vertical and horizontal velocity for a particle pair settling in a homogeneous fluid, are presented here for completion. We modify the terms presented in Kynch [35] such that the particles have equal diameter, as in the case in our study.

$$K = 1 - 2\tilde{s}^6 Q, \tag{B1a}$$

$$L = -\frac{15}{4}\tilde{s}^4 P\left(1 - \frac{8}{5}\tilde{s}^2\right), \tag{B1b}$$

$$M = \frac{1}{4}(3 + 2\tilde{s}^2) + \frac{8}{5}\tilde{s}^{10} Q(5 - 16\tilde{s}^2), \tag{B1c}$$

$$N = \frac{3}{4}(1 - 2\tilde{s}^2) + \frac{3}{8}\tilde{s}^6\left(10P\left(1 - \frac{8}{5}\tilde{s}^2\right)^2(5 - 12\tilde{s}^2) - Q\frac{64}{15}\tilde{s}^4(5 - 16\tilde{s}^4)\right), \tag{B1d}$$

$$\text{where } P = \left[1 - \tilde{s}^6(5 - 12\tilde{s}^2)\right]^{-1}, \tag{B1e}$$

$$Q = \left[1 - \frac{1}{4}\tilde{s}^6(5 - 16\tilde{s}^2)\right]^{-1}. \tag{B1f}$$

[1] S. W. Fowler and G. A. Knauer, Role of large particles in the transport of elements and organic compounds through the oceanic water column, Prog. Oceanogr. **16**, 147 (1986).
[2] S. MacIntyre, A. L. Alldredge, and C. C. Gotschalk, Accumulation of marines now at density discontinuities in the water column, Limnol. Oceanogr. **40**, 449 (1995).
[3] J. C. Prairie, K. Ziervogel, C. Arnosti, R. Camassa, C. Falcon, S. Khatri, R. M. McLaughlin, B. L. White, and S. Yu, Delayed settling of marine snow at sharp density transitions driven by fluid entrainment and diffusion-limited retention, Mar. Ecol.: Prog. Ser. **487**, 185 (2013).
[4] J. C. Prairie, K. Ziervogel, R. Camassa, R. M. McLaughlin, B. L. White, C. Dewald, and C. Arnosti, Delayed settling of marine snow: Effects of density gradient and particle properties and implications for carbon cycling, Mar. Chem. **175**, 28 (2015).
[5] C. M. Andersen and T. G. Nielsen, The effect of a sharp pycnocline on plankton dynamics in a freshwater influenced Norwegian fjord, Ophelia **56**, 135 (2002).
[6] D. Kaiser, N. Kowalski, and J. J. Waniek, Effects of biofouling on the sinking behavior of microplastics, Environ. Res. Lett. **12**, 124003 (2017).
[7] L. Khatmullina and I. Isachenko, Settling velocity of microplastic particles of regular shapes, Mar. Pollut. Bull. **114**, 871 (2017).
[8] I. Chubarenko, E. Esiukova, A. Bagaev, I. Isachenko, N. Demchenko, M. Zobkov, I. Efimova, M. Bagaeva, and L. Khatmullina, Behavior of microplastics in coastal zones, in *Microplastic Contamination in Aquatic Environments* (Elsevier, Amsterdam, Netherlands, 2018), pp. 175–223.
[9] J. D. Parsons, J. W. M. Bush, and J. P. M. Syvitski, Hyperpycnal plume formation from riverine outflows with small sediment concentrations, Sedimentology **48**, 465 (2001).
[10] B. R. Sutherland, M. K. Gingras, C. Knudson, L. Steverango, and C. Surma, Particle-bearing currents in uniform density and two-layer fluids, Phys. Rev. Fluids **3**, 023801 (2018).
[11] J. Magnaudet and M. J. Mercier, Particles, drops, and bubbles moving across sharp interfaces and stratified layers, Annu. Rev. Fluid Mech. **52**, 61 (2020).
[12] F. Blanchette, Mixing and convection driven by particles settling in temperature- stratified ambients, Int. J. Heat Mass Transf. **56**, 732 (2013).
[13] I. A. Houghton, J. R. Koseff, S. G. Monismith, and J. O. Dabiri, Vertically migrating swimmers generate aggregation-scale eddies in a stratified column, Nature **556**, 497 (2018).
[14] K. Y. Yick, C. R. Torres, T. Peacock, and R. Stocker, Enhanced drag of a sphere settling in a stratified fluid at small Reynolds numbers, J. Fluid Mech. **632**, 49 (2009).
[15] J. Zhang, M. J. Mercier, and J. Magnaudet, Core mechanisms of drag enhancement on bodies settling in a stratified fluid, J. Fluid Mech. **875**, 622 (2019).
[16] C. R. Torres, H. Hanazaki, J. Ochoa, J. Castillo, and M. Van Woert, Flow past a sphere moving vertically in a stratified diffusive fluid, J. Fluid Mech. **417**, 211 (2000).
[17] D. E. Mowbray and B. S. H. Rarity, The internal wave pattern produced by a sphere moving vertically in a density stratified liquid, J. Fluid Mech. **30**, 489 (1967).
[18] K. Kindler, A. Khalili, and R. Stocker, Diffusion-limited retention of porous particles at density interfaces, Proc. Natl. Acad. Sci. **107**, 22163 (2010).
[19] M. Panah, F. Blanchette, and S. Khatri, Simulations of a porous particle settling in a density-stratified ambient fluid, Phys. Rev. Fluids **2**, 114303 (2017).
[20] A. N. Srdić-Mitrović, N. A. Mohamed, and H. J. S. Fernando, Gravitational settling of particles through density interfaces, J. Fluid Mech. **381**, 175 (1999).
[21] R. Camassa, C. Falcon, J. Lin, R. M. McLaughlin, and N. Mykins, A first-principle predictive theory for a sphere falling through sharply stratified fluid at low Reynolds number, J. Fluid Mech. **664**, 436 (2010).
[22] N. Abaid, D. Adalsteinsson, A. Agyapong, and R. M. McLaughlin, An internal splash: Levitation of falling spheres in stratified fluids, Phys. Fluids **16**, 1567 (2004).
[23] L. Verso, M. van Reeuwijk, and A. Liberzon, Transient stratification force on particles crossing a density interface, Int. J. Multiphase Flow **121**, 103109 (2019).
[24] C. Darwin, Note on hydrodynamics, Math. Proc. Cambridge Philos. Soc. **49**, 342 (1953).
[25] I. Eames, S. E. Belcher, and J. C. R. Hunt, Drift, partial drift and Darwin's proposition, J. Fluid Mech. **275**, 201 (1994).

[26] B. G. Inman, C. J. Davies, C. R. Torres, and P. J. S. Franks, Deformation of ambient chemical gradients by sinking spheres, J. Fluid Mech. **892**, A33 (2020).
[27] A. Doostmohammadi, S. Dabiri, and A. M. Ardekani, A numerical study of the dynamics of a particle settling at moderate Reynolds numbers in a linearly stratified fluid, J. Fluid Mech. **750**, 5 (2014).
[28] A. M. Ardekani and R. H. Rangel, Numerical investigation of particle-particle and particle-wall collisions in a viscous fluid, J. Fluid Mech. **596**, 437 (2008).
[29] W.-P. P. Breugem, A second-order accurate immersed boundary method for fully resolved simulations of particle-laden flows, J. Comput. Phys. **231**, 4469 (2012).
[30] M. Coquerelle and G.-H. H. Cottet, A vortex level set method for the two-way coupling of an incompressible fluid with colliding rigid bodies, J. Comput. Phys. **227**, 9121 (2008).
[31] S. M. M. Dash and T. S. S. Lee, Two spheres sedimentation dynamics in a viscous liquid column, Comput. Fluids **123**, 218 (2015).
[32] R. Glowinski, T. W. W. Pan, T. I. I. Hesla, D. D. D. Joseph, and J. Périaux, A fictitious domain approach to the direct numerical simulation of incompressible viscous flow past moving rigid bodies: Application to particulate flow, J. Comput. Phys. **169**, 363 (2001).
[33] M. S. Smoluchowski, On the practical applicability of Stokes' law of resistance, and the modifications of it required in certain cases, in *Proceedings of the Fifth International Congress of Mathematicians* (Cambridge University Press, London, 1912), p. 192.
[34] M. Stimson and G. B. Jeffery, The motion of two spheres in a viscous fluid, Proc. R. Soc. London A **111**, 110 (1926).
[35] G. J. Kynch, The slow motion of two or more spheres through a viscous fluid, J. Fluid Mech. **5**, 193 (1959).
[36] A. J. Goldman, R. G. Cox, and H. Brenner, The slow motion of two identical arbitrarily oriented spheres through a viscous fluid, Chem. Eng. Sci. **21**, 1151 (1966).
[37] G. F. Eveson, E. W. Hall, and S. G. Ward, Interaction between two equal-sized equal-settling spheres moving through a viscous liquid, Br. J. Appl. Phys. **10**, 43 (1959).
[38] E. H. Steinberger, H. R. Pruppacher, and M. Neiburger, On the hydrodynamics of pairs of spheres falling along their line of centres in a viscous medium, J. Fluid Mech. **34**, 809 (1968).
[39] A. Doostmohammadi and A. M. Ardekani, Interaction between a pair of particles settling in a stratified fluid, Phys. Rev. E **88**, 023029 (2013).
[40] M. Uhlmann, An immersed boundary method with direct forcing for the simulation of particulate flows, J. Comput. Phys. **209**, 448 (2005).
[41] E. Biegert, B. Vowinckel, and E. Meiburg, A collision model for grain-resolving simulations of flows over dense, mobile, polydisperse granular sediment beds, J. Comp. Phys. **340**, 105 (2017).
[42] T. Kempe and J. Fröhlich, An improved immersed boundary method with direct forcing for the simulation of particle laden flows, J. Comput. Phys. **231**, 3663 (2012).
[43] R. Ouillon, I. A. A. Houghton, J. O. Dabiri, and E. Meiburg, Active swimmers interacting with stratified fluids during collective vertical migration, J. Fluid Mech. **902**, A23 (2020).
[44] M. N. Ardekani, L. A. Asmar, F. Picano, and L. Brandt, Numerical study of heat transfer in laminar and turbulent pipe flow with finite-size spherical particles, Int. J. Heat Fluid Flow **71**, 189 (2018).
[45] F. Blanchette and A. M. Shapiro, Drops settling in sharp stratification with and without Marangoni effects, Phys. Fluids **24**, 042104 (2012).
[46] H. Hanazaki, K. Kashimoto, and T. Okamura, Jets generated by a sphere moving vertically in a stratified fluid, J. Fluid Mech. **638**, 173 (2009).
[47] J. Happel and R. Pfeffer, The motion of two spheres following each other in a viscous fluid, AIChE J. **6**, 129 (1960).
[48] See Supplemental Material at http://link.aps.org/supplemental/10.1103/PhysRevFluids.6.044304 for a video of the particle pair settling in the configurations shown in Fig. 4.
[49] R. Camassa, C. Falcon, J. Lin, R. M. McLaughlin, and R. Parker, Prolonged residence times for particles settling through stratified miscible fluids in the Stokes regime, Phys. Fluids **21**, 031702 (2009).
[50] F. Blanchette and J. W. M. Bush, Particle concentration evolution and sedimentation-induced instabilities in a stably stratified environment, Phys. Fluids **17**, 073302 (2005).

[51] M. Bayareh, A. Doostmohammadi, S. Dabiri, and A. M. Ardekani, On the rising motion of a drop in stratified fluids, Phys. Fluids **25**, 103302 (2013).
[52] S. Dabiri, A. Doostmohammadi, M. Bayareh, and A. M. M. Ardekani, Rising motion of a swarm of drops in a linearly stratified fluid, Int. J. Multiphase Flow **69**, 8 (2015).
[53] A. F. Fortes, D. D. Joseph, and T. S. Lundgren, Nonlinear mechanics of fluidization of beds of spherical particles, J. Fluid Mech. **177**, 467 (1987).
[54] G. W. Slack, Sedimentation of compact clusters of uniform spheres, Nature **200**, 466 (1963).
[55] R. Mehaddi, F. Candelier, and B. Mehlig, Inertial drag on a sphere settling in a stratified fluid, J. Fluid Mech. **855**, 1074 (2018).
[56] N. Mordant and J.-F. Pinton, Velocity measurement of a settling sphere, Eur. Phys. J. B **18**, 343 (2000).
[57] A. ten Cate, C. H. Nieuwstad, J. J. Derksen, and H. E. A. Van den Akker, Particle imaging velocimetry experiments and lattice-Boltzmann simulations on a single sphere settling under gravity, Phys. Fluids **14**, 4012 (2002).
[58] Ankit Rohatgi, Webplotdigitizer: Version 4.4 (2020), https://automeris.io/WebPlotDigitizer.